Pergamon

PII: S1359-6454(96)00366-7

Acta mater. Vol. 45, No. 6, pp. 2247–2255, 1997

Published by Elsevier Science Ltd

1359-6454/97 $17.00 + 0.00

MONTE CARLO SIMULATION OF EFFECTIVE ELASTIC CONSTANTS OF POLYCRYSTALLINE THIN FILMS

R. L. MULLEN[1], R. BALLARINI[1], Y. YIN[1] and A. H. HEUER[2]

[1]Department of Civil Engineering, and [2]Department of Materials Science and Engineering, Case Western Reserve University, Cleveland, Ohio 44106-7204, U.S.A.

(Received 22 May 1996; accepted 8 October 1996)

Abstract—A Monte Carlo finite element model is developed for predicting the scatter in the nominal elastic constants of a thin film aggregate of cubic crystals. Universal results for the nominal plane strain Young's modulus and Poisson's ratio are presented as functions of the number of grains within a unit volume, and two parameters that quantify the level of the crystalline anisotropy. The predictions are compared with formulae that are derived for plane strain Voigt and Reuss bounds. © *1997 Acta Metallurgica Inc.*

INTRODUCTION

Typical stress analyses of engineered structures rely on the assumption that the constituent materials are homogeneous, and in most cases, isotropic. These approximations have proved to be appropriate for structures whose characteristic dimensions are much larger than those of the material microstructure (steel and concrete buildings, for example). However, they may be inappropriate for structures whose characteristic dimensions are of the same order as those of the microstructure, e.g. microelectromechanical systems (MEMS) devices. The principal material used to fabricate most current MEMS devices is polycrystalline silicon, which is comprised of anisotropic single crystals possessing "cubic" symmetry. The random directions of the principal material axes within each grain result in an inhomogeneous polycrystalline structure. Predicting the scatter in the nominal elastic constants of structures comprised of polycrystalline silicon motivated the development of the model presented in this paper, which can be easily modified to analyse general anisotropy.

Determining the average elastic and plastic properties of polycrystalline materials has been the focus of much research during the past 50 years. Before the advent of the computer, analytical models relied on simplifying assumptions regarding the interactions of individual crystals as well as their shape. As far as the authors know, the first analytical model for an aggregate of cubic crystals was proposed by Hershey [1]. Christensen [2] has provided an excellent critique of different classes of analytical models for predicting the elastic and inelastic response of composite materials. A practical limitation of these models is that they do not provide estimates for the scatter of the properties from their mean value, as functions of the number of grains within a unit volume. This information may be very important in certain applications. For example, specifications for disposable blood pressure sensors require 1% accuracy in pressure readings [3], which translates into at most 1% accuracy in predicted deflections, and hence elastic moduli. Currently this performance is achieved by using bulk micromachined single crystal silicon. Surface micromachining provides more flexibility in geometric design, but uses polycrystalline silicon. If this material is to be used in applications that require precise predictions of mechanical response, then a quantitative understanding of the scatter in its elastic moduli that results from the inhomogeneity of the microstructure is paramount. To estimate the dispersion in elastic constants accurately, one needs to perform analyses that model the microstructure explicitly.

This paper presents a Monte Carlo simulation that predicts the nominal elastic constants and their coefficient of variation of thin films comprised of a finite assembly of cubic crystals. Such structures are ubiquitous in MEMS applications. Figure 1(a) shows a fracture device that is being used by the authors [4] to study fatigue and fracture of polycrystalline silicon. The average diameter of the grains is about 1 μm, as seen in the cross-sectional TEM image shown in Fig. 1(b) and in the planar view micrograph of Fig. 1(c); it is clear that the microstructure of such devices is (nearly) columnar. This supports the plane strain finite element analysis which is presented in the next section. The analysis relies on a Voronoi tessellation of the microstructure, and follows the approach taken by Kumar [5], who focused on comparing, for a large number of grains, the predictions from this model with those derived from available analytical models.

FORMULATION

With respect to the global coordinate system x–y–z shown in Fig. 2, the thin film is analysed under plane strain conditions, $u_z = \partial()/\partial z = 0$, where u_z is the displacement in the z direction, and () denotes any physical quantity. For a given number of grains n, the topology of the microstructure within the unit volume shown in Fig. 2 is approximated, for each of m simulations, as a Voronoi tessellation. The tessellation is constructed by first generating, using a Poisson process, a set of random nucleus points $\vec{r}_i$ $(i = 1, n)$. The set of all points that are closer to $\vec{r}_i$ than to any other nucleus $\vec{r}_j$ $(i \neq j)$ comprises the ith Voronoi cell. The assembly of the n convex, planar

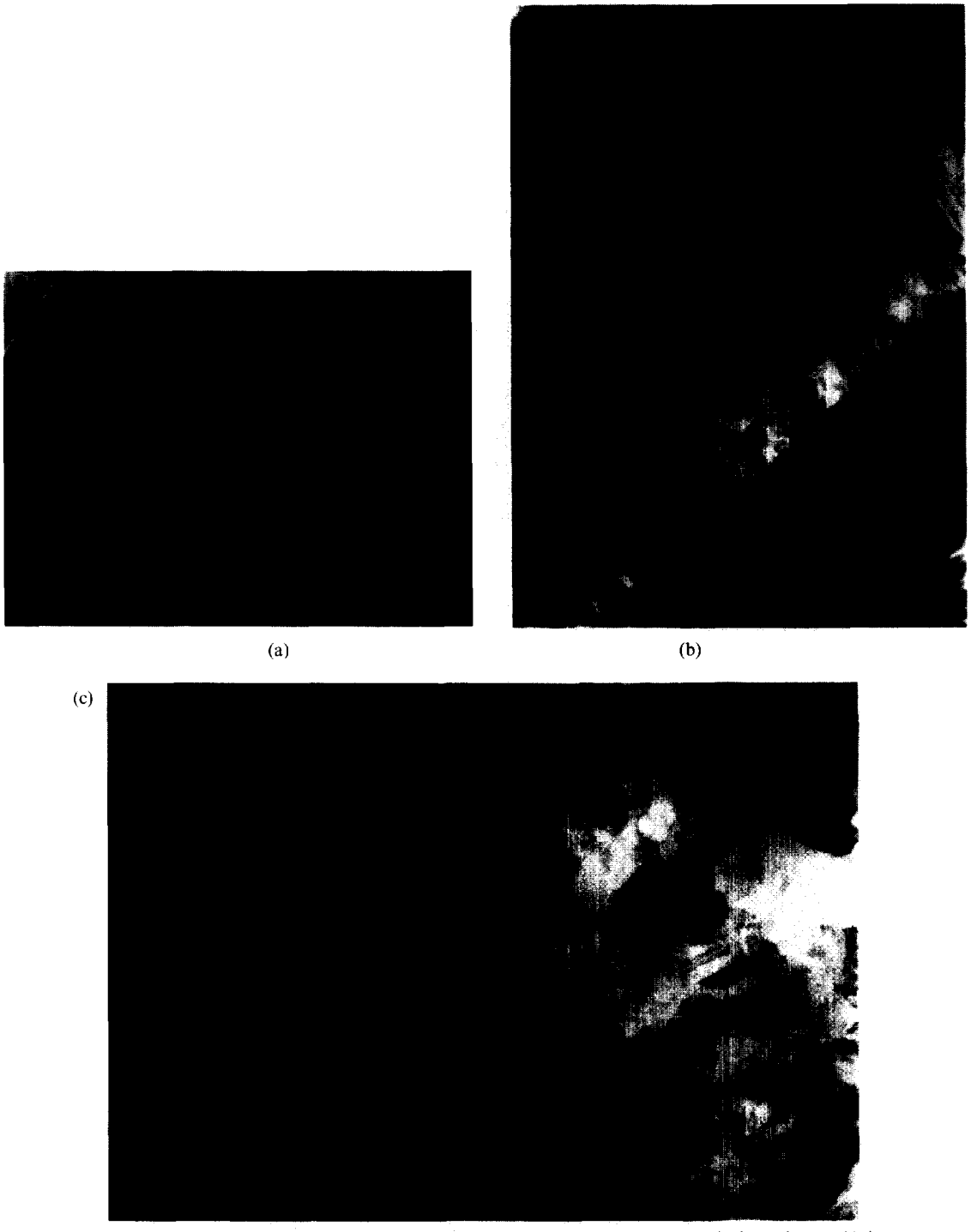

Fig. 1. Microstructure of polysilicon microfracture specimens; (a) shows a typical specimen, (b) is a cross-sectional transmission electron micrograph (TEM) of a boron-doped chemical vapor deposition film; and (c) shows a planar view micrograph of the grain and twin boundaries present in an as-fabricated undoped microdevice.

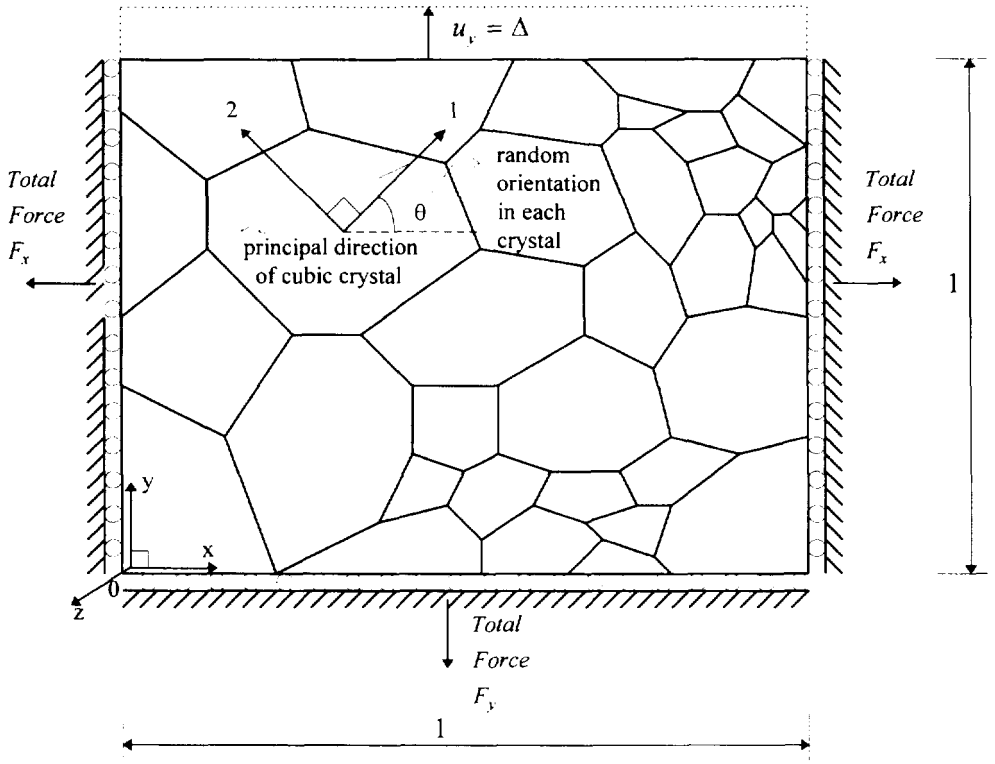

Fig. 2. Voronoi tessellation of microstructure for n-grains (n = 5–1000).

edged cells defines the tessellation. Each grain is discretized with a sufficient number of quadratic displacement finite elements. The details of the algorithm used to construct the tessellation and the finite element method solution procedure can be found in Ref. [6].

Each grain is assumed to possess cubic symmetry. With respect to the local coordinates axes 1–2 shown in Fig. 2, which represent the principal material directions of a typical grain, the stress–strain relations are given, in matrix and component form, by Hooke's law for a cubic material in plane strain:

$$\{\sigma\} \equiv \begin{Bmatrix} \sigma_{11} \\ \sigma_{22} \\ \sigma_{12} \end{Bmatrix} = [C]\{\epsilon\} \equiv \begin{bmatrix} c_{11} & c_{12} & 0 \\ c_{12} & c_{11} & 0 \\ 0 & 0 & 2c_{44} \end{bmatrix} \begin{Bmatrix} \epsilon_{11} \\ \epsilon_{22} \\ \epsilon_{12} \end{Bmatrix} \quad (1)$$

where σ_{ij} and ϵ_{ij} $(i, j = 1, 2)$ are, respectively, components of the symmetric stress and strain tensors. System 1–2 is rotated through an angle θ from the global x-axis. The requirement that the strain energy be positive definite places the following restrictions on the elastic constants:

$$c_{11} > 0 \quad c_{11}^2 - c_{12}^2 > 0 \quad c_{44} > 0. \quad (2)$$

The level of anisotropy is quantified by the parameters A and $\bar{\nu}$, defined as

$$A \equiv \frac{2c_{44}}{c_{11} - c_{12}} \quad (3a)$$

$$\bar{\nu} \equiv \frac{c_{12}}{c_{11} + c_{12}}. \quad (3b)$$

The combination $(c_{11} - c_{12})/2$ represents the shear modulus associated with the shear strain of an element whose normals are rotated 45° with respect to the principal directions, while $\bar{\nu}$ is the apparent plane strain Poisson's ratio associated with uniaxial loading along the principal directions. For isotropic materials $A = 1$ and $\bar{\nu} = \nu$, where ν is Poisson's ratio. The randomness of the orientation of the principal directions is introduced by assigning, to each cell, a uniformly distributed random angle θ.

The thin film structure is loaded, as shown in Fig. 2, through the following boundary conditions:

$$u_y = \Delta, \quad y = 1 \quad (4a)$$

$$u_x = \sigma_{xy} = 0, \quad x = 0, \quad x = 1 \quad (4b)$$

$$u_y = \sigma_{xy} = 0, \quad y = 0. \quad (4c)$$

These are associated with nominal (average) strain components $\epsilon_{yy}^n = \Delta/1$, $\epsilon_{xx}^n = 0$, $\epsilon_{xy}^n = 0$. The finite element method is used to calculate the total reaction forces (per unit thickness) F_x and F_y shown in Fig. 2, which for the unit length edges, correspond to nominal stress components σ_{xx}^n and σ_{yy}^n, respectively. The associated nominal values of the Poisson's ratio ν^n and plane strain Young's modulus $\bar{E}^n \equiv E^n/[1 - (\nu^n)^2]$ are defined by invoking Hooke's law for the isotropic continuum under plane strain

conditions:

$$\begin{Bmatrix} \sigma_{xx}^n = F_x \\ \sigma_{yy}^n = F_y \\ \sigma_{xy}^n = 0 \end{Bmatrix} = \frac{E^n}{(1+\nu^n)(1-2\nu)}$$

$$\begin{bmatrix} 1-\nu^n & \nu^n & 0 \\ \nu^n & 1-\nu^n & 0 \\ 0 & 0 & (1-2\nu^n) \end{bmatrix} \begin{Bmatrix} \epsilon_{xx}^n = 0 \\ \epsilon_{yy}^n = \Delta \\ \epsilon_{xy}^n = 0 \end{Bmatrix}. \quad (5)$$

Equations (5) provide

$$\nu^n = \frac{1}{1 + \frac{F_y}{F_x}} \quad (6a)$$

$$\bar{E}^n = \frac{E^n}{[1-(\nu^n)^2]} = \frac{(1+\nu^n)(1-2\nu^n)}{\nu^n[1-(\nu^n)^2]} \frac{F_x}{\Delta}. \quad (6b)$$

The steps described above are repeated m times for each value of n.

VOIGT AND REUSS BOUNDS FOR PLANE STRAIN

The plane strain elastic constants defined as Reuss bounds are isotropic within the plane and are calculated by averaging the single crystal stiffness matrix over all possible orientations of the random angle θ. The average stiffness matrix is calculated as

$$[C]^{\text{Reuss}} \equiv \frac{1}{2\pi} \int_0^{2\pi} [T]^{\text{T}}[C][T]\, \mathrm{d}\theta \quad (7)$$

where matrix $[T]$ and its transpose $[T]^{\text{T}}$, which transform the stiffness matrix from principle axes to those rotated by angle θ, are defined by

$$[T] \equiv \begin{bmatrix} \cos^2\theta & \sin^2\theta & \cos\theta\sin\theta \\ \sin^2\theta & \cos^2\theta & -\cos\theta\sin\theta \\ -2\cos\theta\sin\theta & 2\cos\theta\sin\theta & \cos^2\theta - \sin^2\theta \end{bmatrix}. \quad (8)$$

Equating the result of the integration in equation (7) with the stiffness matrix in equation (5) provides

$$\nu^{\text{Reuss}} = \frac{c_{11} + 3c_{12} - 2c_{44}}{4(c_{11} + c_{12})} \quad (9a)$$

$$\bar{E}^{\text{Reuss}} = \frac{E^{\text{Reuss}}}{[1-(\nu^{\text{Reuss}})^2]} = \frac{(1+\nu^{\text{Reuss}})}{2[1-(\nu^{\text{Reuss}})^2]}(c_{11} - c_{12} + 2c_{44}). \quad (9b)$$

The plane strain elastic constants defined as Voigt bounds are isotropic within the plane and are calculated by averaging the single crystal compliance matrix over all possible orientations of the random angle θ. The average compliance matrix is calculated as

$$[S]^{\text{Voigt}} \equiv \frac{1}{2\pi} \int_0^{2\pi} [T]^{\text{T}}[C]^{-1}[T]\, \mathrm{d}\theta \quad (10)$$

where the superscript -1 denotes matrix inverse. Equating the result of the integration in equation (10) with the inverse of the stiffness matrix in equation (5) provides

$$\nu^{\text{Voigt}} = -\frac{2s_{11} + 6s_{12} - s_{44}}{2(2s_{11} - 2s_{12} + s_{44})} \quad (11a)$$

$$\bar{E}^{\text{Voigt}} = \frac{E^{\text{Voigt}}}{[1-(\nu^{\text{Voigt}})^2]} = \frac{4(1+\nu^{\text{Voigt}})}{[1-(\nu^{\text{Voigt}})^2](2s_{11} - 2s_{12} + s_{44})} \quad (11b)$$

in which

$$s_{11} \equiv \frac{c_{11}}{c_{11}^2 - c_{12}^2} \quad s_{12} \equiv -\frac{c_{12}}{c_{11}^2 - c_{12}^2} \quad s_{44} \equiv \frac{1}{c_{44}}. \quad (12)$$

RESULTS

Typical results are presented in Fig. 3(a) and (b), which show the scatter in $\bar{E}^n$ for $m = 100$ realizations. Figure 3(a) is for silicon, which is slightly anisotropic with $c_{11} = 2.55c_{12} = 2c_{44} = 160$ GPa ($A = 1.65$, $\bar{\nu} = 0.28$). Figure 3(b) is for cesium, which is highly anisotropic with $c_{11} = 1.30c_{12} = 1.23c_{44} = 5.26$ GPa ($A = 6.98$, $\bar{\nu} = 0.43$). It is observed that even for 1000 grains the scatter is of the order of a few percent. This implies that polysilicon microdevices whose characteristic dimensions are less than ≈ 1 mm cannot be used in designs that rely on a knowledge of the elastic modulus to within a few percent.

The coefficient of variation (COV) of $\bar{E}^n$ of eight cubic materials, defined as

$$\text{COV} \equiv \sqrt{\frac{1}{(m-1)(\bar{E}_{\text{avg}}^n)^2} \sum_m [(\bar{E}^n)^2 - (\bar{E}_{\text{avg}}^n)^2]} \quad (13)$$

is presented in Table 1 as a function of the number of grains in the film. In equation (13) the subscript "avg" denotes the average value of m simulations. The COV for films comprised of 1000 grains for an additional 20 materials are listed in Table 2. These results show that the COV of $\bar{E}^n$ is a strong function of both A and $\bar{\nu}$.

Tables 3 and 4 show that the plane strain Young's modulus and Poisson's ratio predicted by the model for 1000 grains lie within the Voigt and Reuss bounds. The results presented in Table 3 (4) were calculated using $m = 100$ (10).

Figures 4 and 5 show, for $\bar{\nu} = 0.1, 0.2, 0.3, 0.4$, the effects of A on $\bar{E}^n$ and ν^n for $n = 10, 100, 1000$. In these plots $\bar{E}^n$ is normalized with the "isotropic" plane strain Young's modulus $\bar{E}^{\text{isotropic}}$ obtained by equating the first entry in the stiffness matrix for

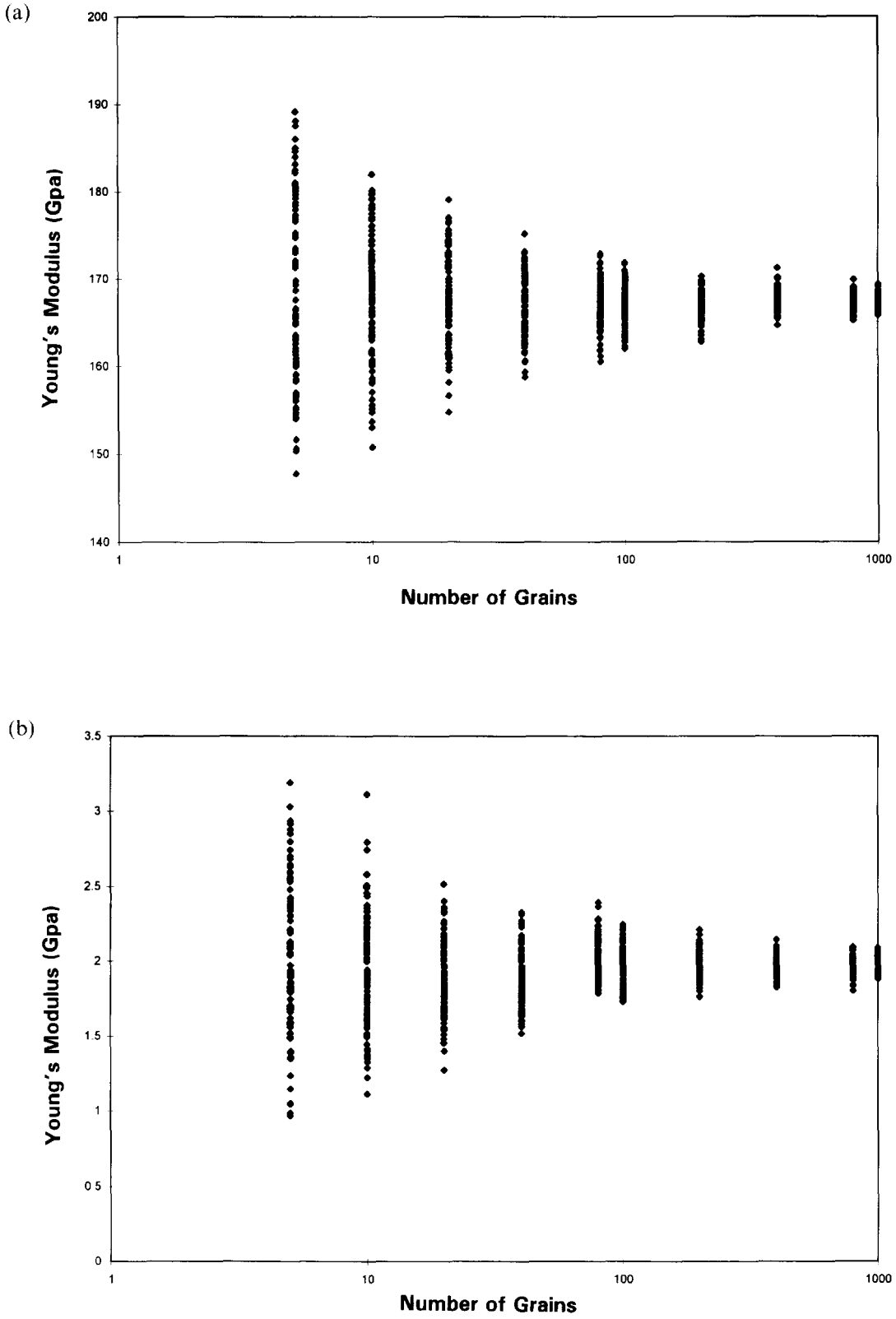

Fig. 3. Scatter of nominal plane strain Young's modulus $\bar{E}^n$ as a function of number of grains n: (a) silicon, (b) cesium.

Table 1. Coefficient of variation of nominal plane strain Young's modulus $\bar{E}^n$ of various cubic materials vs number of grains n ($m = 100$ simulations for each n); $c_{ij} \times 10^{-6}$ Pa shown

Number of cells	Aluminum	Ammonium bromide	Argon	Calcium fluoride	Cesium	Diamond	Gold	Silicon
Character properties	$c_{11} = 108.24$ $c_{12} = 62.16$ $c_{44} = 28.41$ $A = 1.23$ $\bar{\nu} = 0.107$	$c_{11} = 29.60$ $c_{12} = 5.90$ $c_{44} = 5.30$ $A = 0.447$ $\bar{\nu} = 0.166$	$c_{11} = 5.29$ $c_{12} = 1.35$ $c_{44} = 1.59$ $A = 0.807$ $\bar{\nu} = 0.203$	$c_{11} = 162.80$ $c_{12} = 43.30$ $c_{44} = 33.40$ $A = 0.559$ $\bar{\nu} = 0.210$	$c_{11} = 2.59$ $c_{12} = 2.17$ $c_{44} = 1.60$ $A = 7.62$ $\bar{\nu} = 0.456$	$c_{11} = 950.00$ $c_{12} = 390.00$ $c_{44} = 430.00$ $A = 1.54$ $\bar{\nu} = 0.291$	$c_{11} = 194.00$ $c_{12} = 166.00$ $c_{44} = 40.00$ $A = 2.86$ $\bar{\nu} = 0.461$	$c_{11} = 168.00$ $c_{12} = 66.00$ $c_{44} = 84.00$ $A = 1.65$ $\bar{\nu} = 0.282$
5	0.029	0.091	0.026	0.074	0.246	0.047	0.188	0.061
10	0.022	0.069	0.015	0.056	0.205	0.037	0.118	0.041
20	0.014	0.054	0.015	0.037	0.134	0.027	0.085	0.030
40	0.010	0.033	0.008	0.025	0.096	0.018	0.062	0.021
80	0.007	0.023	0.007	0.017	0.065	0.013	0.041	0.015
100	0.006	0.026	0.005	0.015	0.064	0.011	0.035	0.013
200	0.005	0.016	0.004	0.013	0.041	0.009	0.029	0.009
400	0.004	0.012	0.003	0.008	0.032	0.006	0.019	0.007
800	0.002	0.008	0.002	0.006	0.028	0.004	0.013	0.005
1000	0.002	0.008	0.002	0.005	0.023	0.004	0.011	0.004

Table 2. Coefficient of variation of nominal plane strain Young's modulus $\bar{E}^n$ of various cubic materials for $n = 1000$ grains ($m = 10$); $c_{ij} \times 10^{-6}$ Pa shown

Material	c_{11}	c_{12}	c_{44}	A	$\bar{\nu}$	COV
Iron	228.09	133.48	110.86	2.34	0.369	0.007
Lead	47.65	40.28	12.50	3.91	0.458	0.015
Lithium	14.80	14.41	10.80	9.39	0.458	0.026
Magnesium oxide	286.00	87.00	148.00	1.49	0.233	0.003
Magnetite	275.00	104.00	95.50	1.12	0.274	0.001
Molybdenum	479.00	165.80	108.50	0.69	0.257	0.003
Nickel	244.00	158.00	102.00	2.37	0.393	0.013
Niobium	245.60	138.70	29.30	0.55	0.361	0.008
Palladium	234.12	176.14	71.17	2.46	0.429	0.011
Potassium	4.14	3.31	2.63	6.34	0.444	0.027
Pyrite	361.88	−47.96	105.49	0.51	0.153	0.003
Rubidium	2.96	2.44	1.60	6.15	0.492	0.026
Silver	119.92	89.74	43.67	2.89	0.428	0.007
Sodium	5.26	4.04	4.26	6.98	0.434	0.017
Tantalum	266.70	160.80	82.49	1.56	0.376	0.004
Thorium	77.70	48.20	51.10	3.46	0.383	0.011
Tungsten	512.57	205.82	152.67	1.00	0.287	0.000
Uranium carbide	320.00	85.00	64.70	0.55	0.210	0.004
Vanadium	196.00	133.00	67.00	2.13	0.404	0.009
Zinc sulfide	94.41	56.96	43.67	2.33	0.376	0.004

Table 3. Comparison of predicted mean values of plane strain Young's modulus $\bar{E}^n$ and Poisson's ratio ν^n with Voigt and Reuss bounds ($m = 100, n = 1000$)

	Character properties			Voigt		Reuss		Model (1000 grains, 100 simulations)	
Materials	c_{11}	c_{12}	c_{44}	Young's modulus	Poisson's ratio	Young's modulus	Poisson's ratio	Young's modulus	Poisson's ratio
Aluminum	108.24	62.16	28.41	79.0	0.349	78.4	0.351	78.7	0.350
Ammonium bromide	29.60	5.90	5.30	23.1	0.258	20.8	0.294	22.0	0.277
Argon	5.29	1.35	1.59	4.64	0.232	4.60	0.235	4.62	0.234
Calcium fluoride	162.80	43.30	33.40	128	0.274	121	0.292	125	0.284
Cesium	2.59	2.17	1.60	2.63	0.310	1.29	0.422	1.98	0.369
Diamond	950.00	390.00	430.00	928	0.235	901	0.247	913	0.242
Gold	194.00	166.00	40.00	94.0	0.425	74.3	0.442	86.3	0.432
Silicon	168.00	66.00	84.00	172	0.212	165	0.229	168	0.221

cubic symmetry, for $A = 1$ (for fixed $\bar{\nu}$) with that of an isotropic material, i.e.

$$\bar{E}^{\text{isotropic}} \equiv \frac{c_{11}(1+\bar{\nu})(1-2\bar{\nu})}{(1-\bar{\nu})^3}. \tag{14}$$

It is observed that the mean value of the elastic constants is relatively insensitive to the number of grains for the practical range $A < 10$. The predicted values lie between the Voigt and Reuss bounds. It is also interesting to note that negative values of the effective Poisson's ratio are realised as a result of the inherent anisotropy of the constituent grains.

Table 4. Comparison of predicted mean values of plane strain Young's modulus $\bar{E}^n$ and Poisson's ratio ν^n with Voigt and Reuss bounds ($m = 10$, $n = 1000$)

	Character properties			Voigt		Reuss		Model (1000 grains, 10 simulations)	
Materials	c_{11}	c_{12}	c_{44}	Young's modulus	Poisson's ratio	Young's modulus	Poisson's ratio	Young's modulus	Poisson's ratio
Iron	228.09	133.48	110.86	220	0.281	195	0.317	207	0.300
Lead	47.65	40.28	12.50	27.4	0.408	20.1	0.435	25.9	0.414
Lithium	14.80	14.41	10.80	16.0	0.312	1.49	0.487	12.0	0.358
Magnesium oxide	286.00	87.00	148.00	297	0.168	291	0.181	294	0.175
Magnetite	275.00	104.00	95.50	245	0.261	245	0.262	245	0.262
Molybdenum	479.00	165.80	108.50	375	0.294	367	0.301	371	0.298
Nickel	244.00	158.00	102.00	213	0.320	186	0.350	199	0.335
Niobium	245.60	138.70	29.30	136	0.392	126	0.402	132	0.397
Palladium	234.12	176.14	71.17	161	0.378	137	0.400	151	0.388
Potassium	4.14	3.31	2.63	4.33	0.296	2.40	0.404	3.40	0.352
Pyrite	361.88	−47.96	105.49	312	0.006	295	0.056	302	0.035
Rubidium	2.96	2.44	1.60	2.75	0.328	1.54	0.417	2.18	0.373
Silver	119.92	89.74	43.67	91.8	0.360	73.9	0.393	83.9	0.375
Sodium	5.26	4.04	4.26	6.39	0.238	3.48	0.385	4.94	0.320
Tantalum	266.70	160.80	82.49	205	0.342	198	0.349	202	0.345
Thorium	77.70	48.20	51.10	86.5	0.238	67.2	0.318	76.8	0.280
Tungsten	512.57	205.82	152.67	429	0.287	429	0.287	429	0.287
Uranium carbide	320.00	85.00	64.70	251	0.275	236	0.294	244	0.284
Vanadium	196.00	133.00	67.00	152	0.350	136	0.370	145	0.360
Zinc sulfide	94.41	56.96	43.67	88.3	0.294	77.9	0.327	83.4	0.310

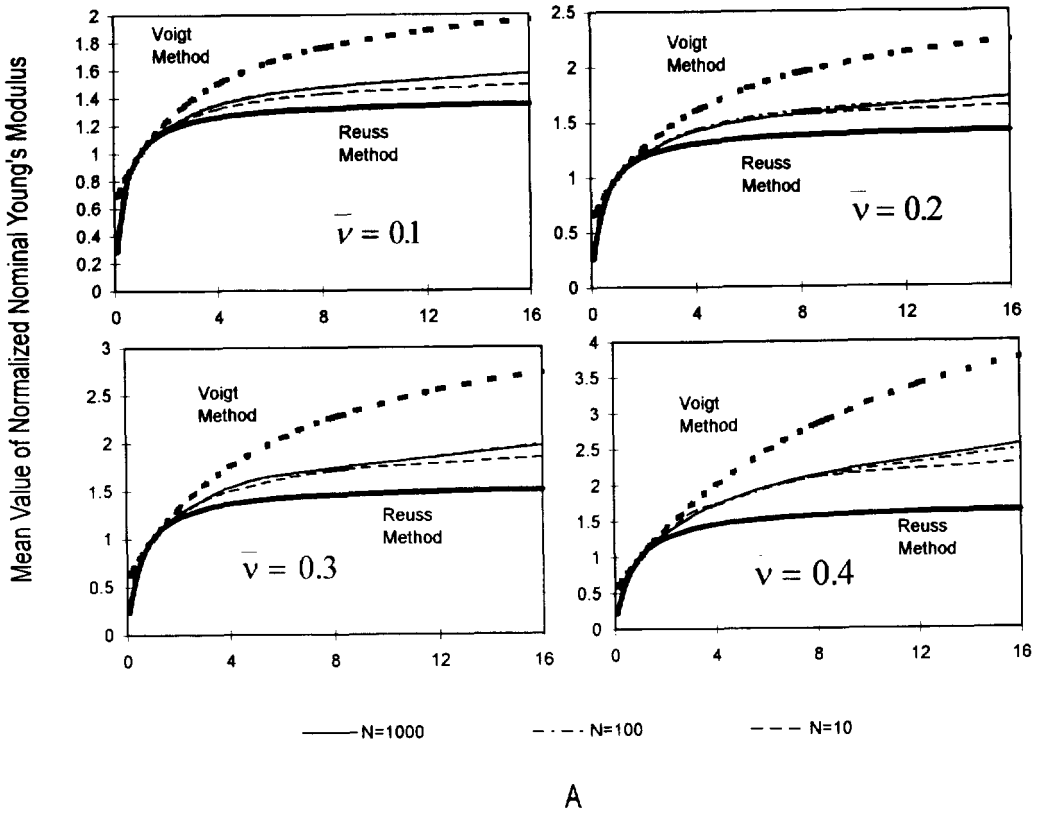

Fig. 4. Mean value of normalized nominal plane strain Young's modulus $\bar{E}^n/\bar{E}^{\text{isotropic}}$ as a function of anisotropy parameter A.

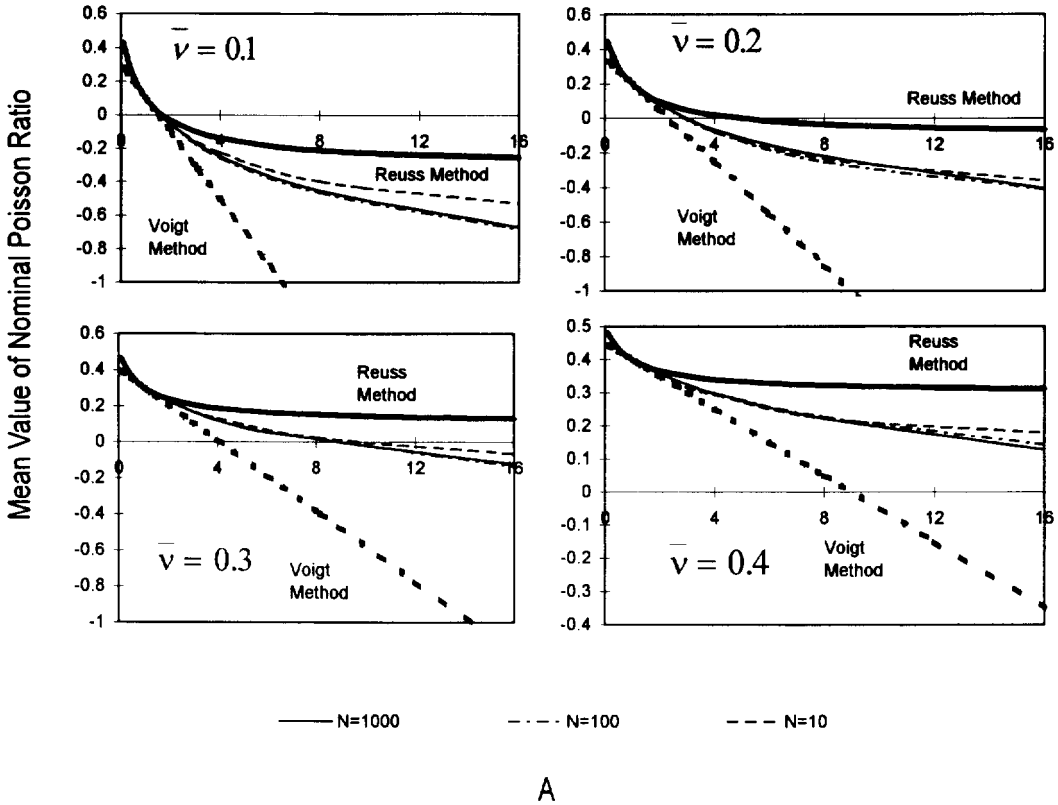

Fig. 5. Mean value of nominal Poisson's ratio ν'' as a function of anisotropy parameter A.

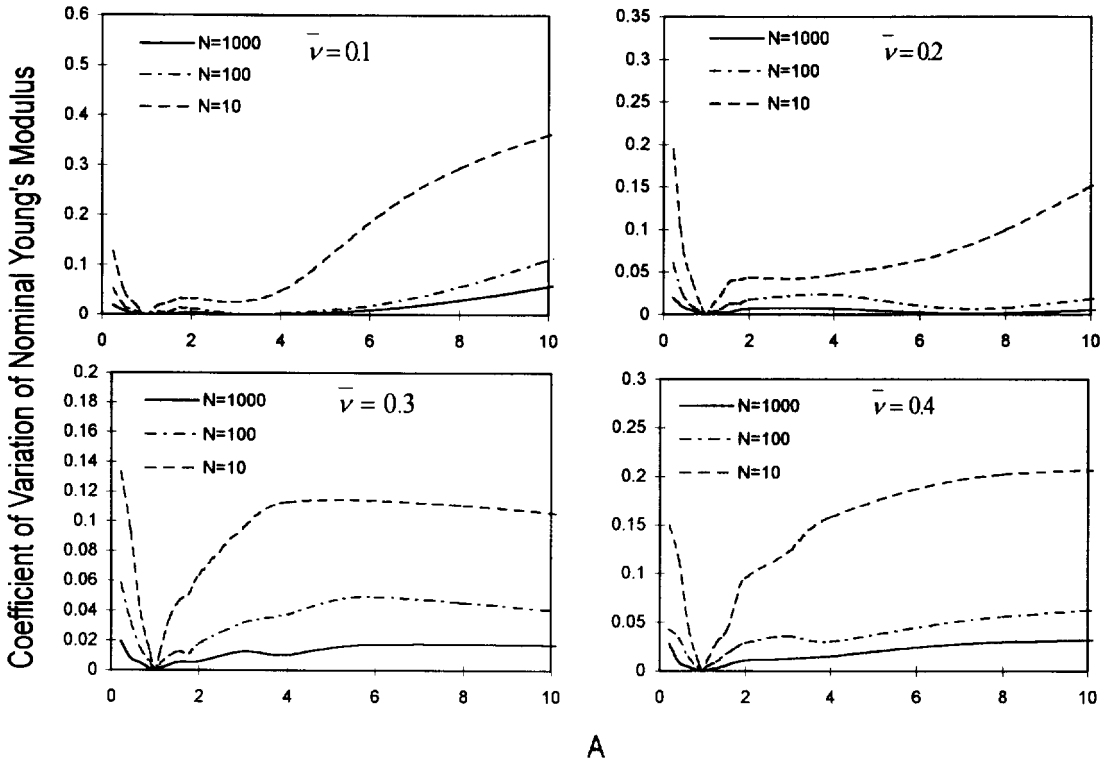

Fig. 6. Coefficient of variation of nominal plane strain Young's modulus $\bar{E}''$ as a function of anisotropy parameter A.

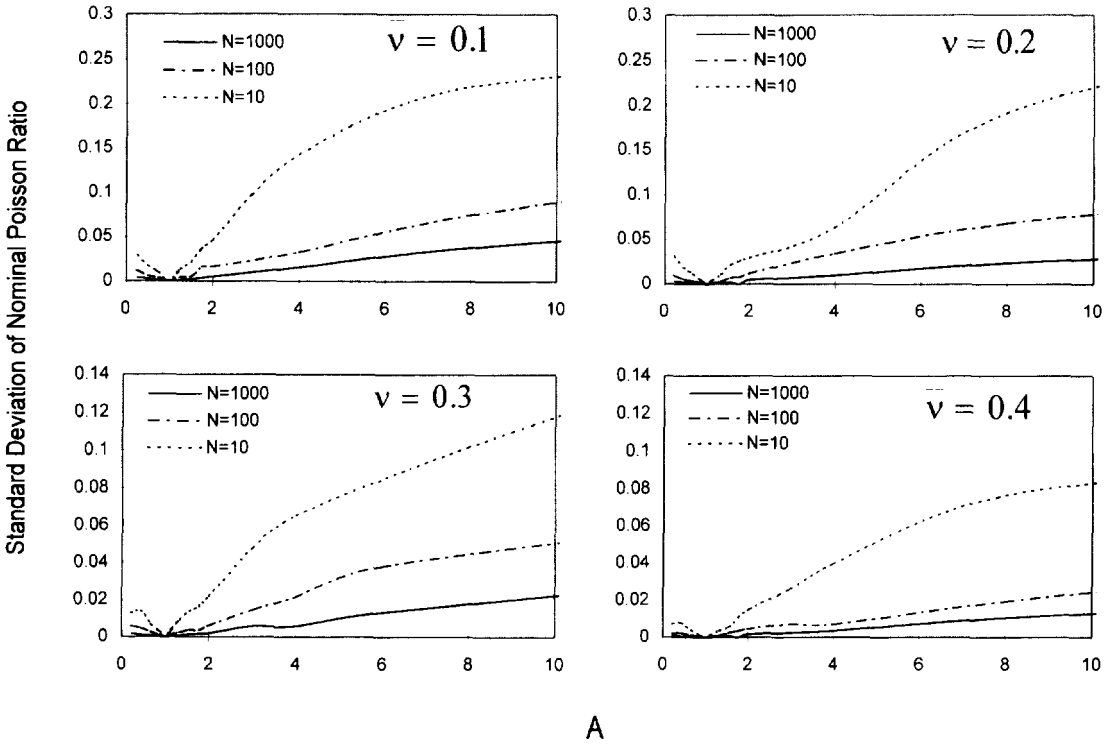

Fig. 7. Standard deviation of nominal Poisson's ratio ν^n as a function of anisotropy parameter A.

Negative Poisson's ratios have been observed experimentally and analytically in materials possessing certain microstructures, as discussed by Lakes [7].

Figure 6(a)–(d) shows, for $\bar{\nu} = 0.1, 0.2, 0.3, 0.4$, the COV of $\bar{E}^n$ as a function of A for $n = 10, 100, 1000$. These plots clearly show that the COV of the nominal Young's modulus is more sensitive to $\bar{\nu}$ than to A.

Figure 7(a)–(d) shows the standard deviation (SD) of ν^n, defined as

$$\mathrm{SD} \equiv \sqrt{\frac{1}{(m-1)} \sum_{m} [(\nu^n)^2 - (\nu^n_{\mathrm{avg}})^2]}. \qquad (15)$$

Figures 6 and 7 can be used to predict the inherent scatter in the nominal plane strain elastic constants of a thin film comprised of a cubic material.

CONCLUSIONS

A finite element-based Monte Carlo has been developed to generate curves that can be used to predict the inherent scatter in the nominal elastic constants of thin films comprised of cubic single crystals. The coefficient of variation of these parameters is a strong function of the two anisotropy parameters $\bar{\nu}$ and A. The numerical results show that the nominal elastic constants are more sensitive to $\bar{\nu}$.

Acknowledgements—This research was funded by the National Science Foundation under Grant MSS94-16752 and by DARPA under Grant DABT 63-92-C-0032.

REFERENCES

1. Hershey, A. V., *ASME J. Appl. Mech.*, 1954, **21**, 236.
2. Christensen, R. M., *J. Mech. Phys. Solids*, 1990, **38**, 379.
3. Bryzek, J., Mayer R. and Barth, P., *IEEE Solid-State Sensor and Actuator Workshop*, IEEE, New York. Hilton Head Island, South Carolina, 6–9 June, 1988, pp. 121–122.
4. Ballarini, R., Mullen, R. L., Yin, Y., Kahn, H., Stemmer, S. and Heuer, A. H., The fracture toughness of polysilicon microdevices: a first report, *J. Mat. Res.* (in press) 1996.
5. Kumar, S., Computer simulation of 3D material microstructure and its application in the determination of mechanical behavior of crystalline materials and engineering structures. Ph.D. thesis, Department of Engineering Science and Mechanics, The Pennsylvania State University, 1992.
6. Yin, Y., Monte Carlo simulation of effective elastic constants of polycrystalline thin films. M.S. thesis, Department of Civil Engineering, Case Western Reserve University, 1996.
7. Lakes, R., *Adv. Mater.*, 1993, **5**, 293.